EPJ Web of Conferences **250**, 05004 (2021) https://doi.org/10.1051/epjconf/202125005004
DYMAT 2021

Effects of elevated temperature on a tungsten alloy at high strain-rate

Ezio Cadoni[1,*], *Matteo* Dotta[1], and *Daniele* Forni[1]

[1]DynaMat SUPSI Laboratory, University of Applied Sciences and Arts of Southern Switzerland, Via Catenazzi 23, 6850 Mendrisio, Switzerland.

Abstract. The effects of elevated temperature at high strain rate of a commercial tungsten alloy were investigated. The tests were carried-out at high strain-rate (from 850 to 2200 1/s) by means of a Split Hopkinson Tension Bar device on round specimens having diameter and gauge length of 2mm and 5 mm, respectively. The thermal conditions were obtained by means of a water-cooled induction heating system on the specimen mounted on the SHTB. The dependence of ultimate tensile strength on temperature was found to decrease, while the failure strain increased with temperature. The strain rate linearly growths with the temperature.

1 Introduction

The tungsten alloys are two-phase composite materials combining the advantageous properties of the tungsten phase and the matrix phase. They possess outstanding physicochemical properties such as high density, high strength, high hardness, good corrosion resistance, high thermal conductivity and wear resistance. Thanks to these characteristics they are widely used in numerous engineering applications in aerospace, machining. Many studies were dedicated to their high strain rate behaviour [1–3], and to the temperature effect [4–7] on mechanical characteristics. This study presents the dynamic tensile behaviour of a commercial tungsten alloy. These alloys are frequently subjected to harsh regimes of strain-rate and often combined with elevated temperature. The main objective of this experimental study is to determine the mechanical response of a commercial tungsten alloy when subjected to high strain-rate in tension at elevated temperature. The tests were carried-out at high strain-rate (from 850 to 2200 1/s) by means of a Split Hopkinson Tension Bar (SHTB) device on round specimens having diameter and gauge length of 2mm and 5 mm, respectively. The thermal conditions were obtained by means of a water-cooled induction heating system on the specimen mounted on the SHTB.

2 Material and specimens

The material used in the current study is a commercial tungsten alloy characterised by high-density ($\rho = 16'925\, kg/m^3$) with the chemical composition reported in Table 1. The high strain-rate tests were performed on a round specimen having a diameter of 2mm and gauge

*e-mail: ezio.cadoni@supsi.ch

Table 1. Chemical composition of the commercial Tungsten alloy in wt.%.

C	Co	Ni	O	W
4.20	3.79	7.98	2.59	Balanced

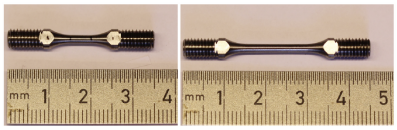

Figure 1. Specimen geometry for dynamic test (left) and quasi-static test (right).

length of 5mm. For the quasi-static tests the specimen had same diameter but longer gauge length (15mm) as shown in Fig. 1. The specimen ends had a M5 fillet for the connection to the testing machines.

3 Experimental set-up

3.1 Quasi-static regime

The reference tests under quasi-static condition (0.001 s^{-1}) were conducted on a Zwick/Roell-Z50 universal testing machine (with 50 kN maximum load bearing capacity) under strain control by means of high precision displacement transducer (with $0.3\mu m$ resolution), see Figure 2a. The tests were performed on specimen with diameter and gauge length of 2mm and 15mm, respectively. In Figure 2b are reported the quasi-static results in terms of stress versus strain curves as well as are indicated elastic modulus (E), proof strength ($R_{0.2}$), ultimate tensile stress (R_m), uniform strain (ϵ_u), fracture stress (f_f), fracture strain (ϵ_f), reduction of area (Z) and modulus of resilience and toughness (W_u and W_f). This tungsten alloy behaves as a quasi-perfect elastic-plastic material even if shows a very limited elongation and brittle failure. In this regime it shows high repeatability [8].

3.2 High strain-rate regime

In order to study the high strain-rate behaviour of this Tungsten alloy a Split Hopkinson Tensile Bar (SHTB) ([9, 10]) was used. This apparatus is composed by two circular straight high strength steel bars with a diameter of 10 mm and a length of 9 and 6 m ([11–13]). The longer bar is used partially used (6 m) as a pretensioned bar and the rest (3 m) as input bar. The second bar is used as output bar. The tungsten alloy specimen is screwed in the input and output bars. By pulling the pretensioned bar by means of a hydraulic jack it is possible to store elastic energy in it and rules the testing velocity as a function of the load amplitude. Both input and output bars are instrumented with semiconductor strain gauges able to measure the incident (ϵ_I), reflected (ϵ_R) and transmitted (ϵ_T) pulses acting on the cross section of the specimen. By applying the one-dimensional elastic plane stress wave propagation theory the engineering value of stress (1), strain (2) and strain-rate (3) are obtained in function of time:

$$\sigma_e(t) = E_0 \cdot \frac{A_0}{A} \cdot \epsilon_T(t) \tag{1}$$

$$\epsilon_e(t) = -\frac{2C_0}{L} \int_0^t \epsilon_R(t) \tag{2}$$

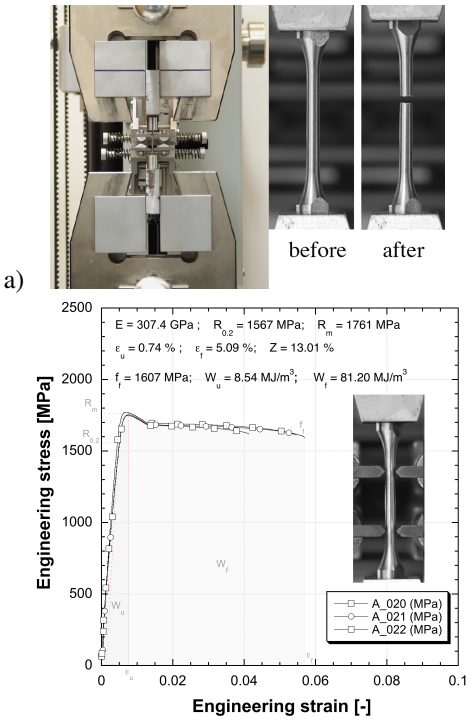

Figure 2. Quasi-static testing: a) set-up; b) results.

$$\dot{\epsilon}_e(t) = -\frac{2C_0}{L} \cdot \epsilon_R(t) \tag{3}$$

The tests at elevated temperatures [14, 15] have been carried out equipping the SHTB with an Ambrell compact EASYHEAT induction water-cooled heating system with maximum power of 2.4 kW (see Figure 3a). By means of this non-contact induction heating is possible to supply energy only to the specimen gauge-length (see Figure 3b) with precise power control with 25 W resolution. The specimens were heated at a constant heating rate of about 3 °C/s to the set temperature (800°C, 900°C, 1000°C and 1100°C).

Three target strain-rates were set at 850 s^{-1}, 1400 s^{-1} and 2200 s^{-1} obtained by imposing, at room temperature, a preload of 26 kN, 35 kN and 50 kN, respectively.
During the tests the signals from strain-gauges were acquired by a HBM-Gen2 data acquisition system while the specimens were filmed at high speed by a fast camera IDT- MotionPro Y4-S3 at 43kfps.
Figure 4a shows how the initial conditions were kept constant. In fact, the input signals are the same for all testing temperature.

The elastic modulus at high temperature has not been measured. It can be supposed a linear decrement with increasing the temperature. Observing the strain rate evolution in function of the temperature a linear trend is noted. The strain rate can be evaluated as:

$$\dot{\epsilon}_T = \dot{\epsilon}_{20°C} + \alpha \cdot T \tag{4}$$

where: $\dot{\epsilon}_T$ is the strain rate at the temperature T; $\dot{\epsilon}_{20°C}$ is the strain rate at room temperature; $\alpha = 0.417$ for this alloy.

a) 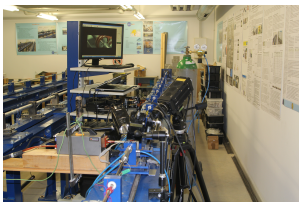 b) 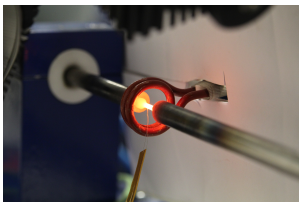

Figure 3. Dynamic testing set-up (a); Sample at elevated temperature in dynamic test (b).

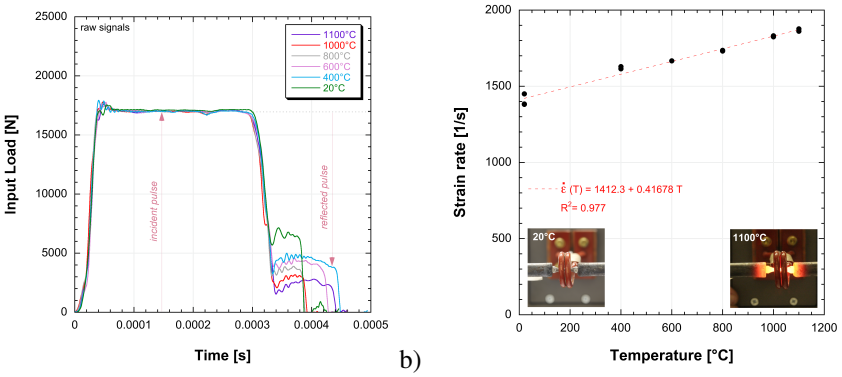

a) b)

Figure 4. Input raw signals at different temperature and same initial loading conditions (a). Strain rate in function of temperature for same initial loading condition (b).

Table 2. Results at 850 1/s.

Temperature (°C)	UTS (MPa)	f_f (MPa)	ϵ_f (%)	$\dot{\epsilon}_{eff.}$ (1/s)
20	2232	2009	5.73	843
800	2198	1136	8.70	1161
900	1044	1007	7.97	1251
1000	964	891	10.70	1295
1100	1254	647	18.13	1290

4 Results

Figures 5a, 5b and 5c show the engineering stress versus strain curves obtained in the temperature range 20 - 1100°C by imposing a preload of 26 kN, 35 kN and 50 kN that causes at ambient temperature a strain rate of 850 s^{-1}, 1400 s^{-1} and 2200 s^{-1}, respectively.

In Tables 2, 3, 4 the average results in terms of ultimate tensile strength (UTS), fracture stress (f_f), fracture elongation (ϵ_f), effective strain rate ($\dot{\epsilon}_{eff.}$) in function of temperature for the three target strain rate are resumed. In Figures 6a,b are reported the reduction cross-area and fracture strain (a) as well as reduction factor of the UTS and fracture stress (b) in function of temperature and 1400 1/s.

Table 3. Results at 1400 1/s.

Temperature (°C)	UTS (MPa)	f_f (MPa)	ϵ_f (%)	$\dot{\epsilon}_{eff.}$ (1/s)
20	2444	2015	5.49	1405
800	2245	1084	8.31	1733
1000	2247	928	9.99	1828
1100	1536	737	16.70	1868

Table 4. Results at 2200 1/s.

Temperature (°C)	UTS (MPa)	f_f (MPa)	ϵ_f (%)	$\dot{\epsilon}_{eff.}$ (1/s)
20	2770	1437	6.7	2200
800	1170	1120	6.45	2495
900	1235	1068	5.7	2540
1000	1351	902	10.17	2595
1100	1067	721	16.07	2610

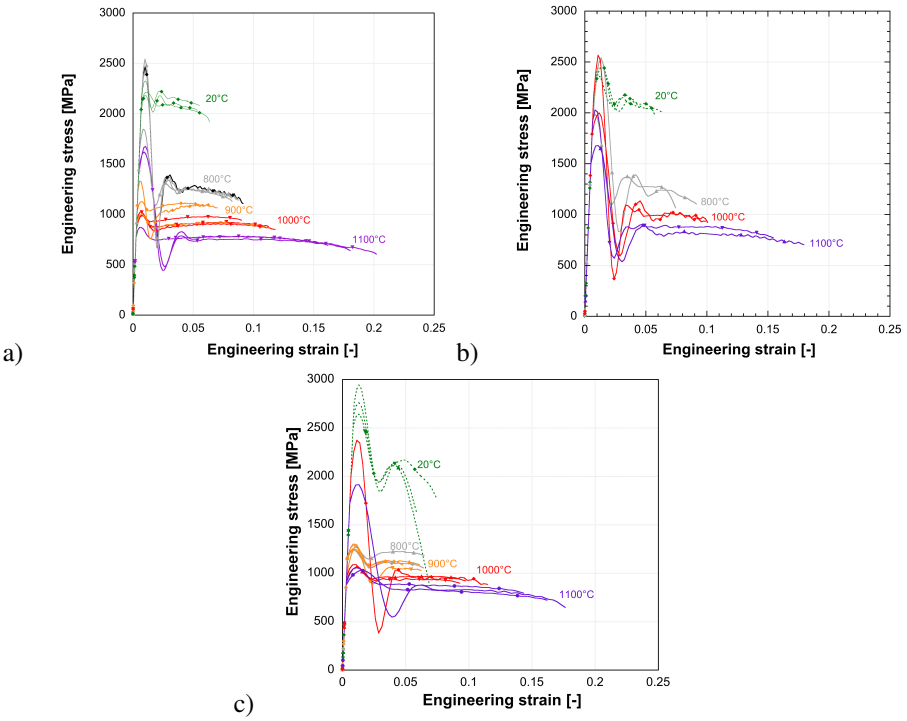

Figure 5. Stress vs. strain at different temperature and (a) 850 1/s, (b) 1400 1/s, (c) 2200 1/s.

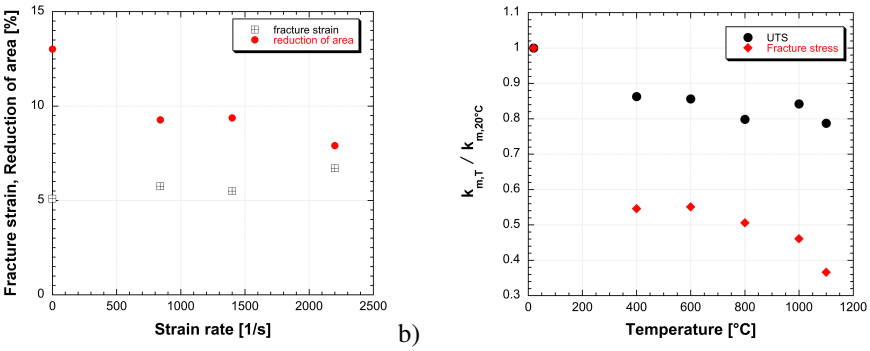

Figure 6. Reduction cross-area and fracture strain (a) and reduction factor of the UTS and fracture stress (b) in function of temperature and 1400 1/s.

5 Conclusions

In this paper, the tensile mechanical properties and fracture behaviour of a commercial Tungsten alloy has been experimentally investigated at elevated temperature ranging from 800 to 1100°C in high strain-rate regime of 850, 1400 and 2200 s^{-1}. It has been found that the tensile mechanical properties such as ultimate tensile strength, fracture strength and nominal total elongation of the examined commercial tungsten alloy depend strongly on the test temperature and generally show a decreasing tendency with increasing temperature.

References

[1] Yadav S., Ramesh K.T. Materials Science and Engineering: A, **203** 140-153 (1995)
[2] Rohr I., Nahme H., Thoma K., Anderson C.E. International Journal of Impact Engineering, **35** 811-819 (2008)
[3] Rittel, D., Weisbrod, G. International Journal of Fracture **112** 87–98 (2001)
[4] Hafizoglu H., Durlu N. International Journal of Impact Engineering, **121** 44-54 (2018)
[5] Wurster S., Gludovatz B., Pippan R. International Journal of Refractory Metals and Hard Materials, **28** 692-697 (2010)
[6] Mutoh Y., Ichikawa K., Nagata K. et al. J. Mat. Sc., 770–775 (1995)
[7] Gong X., Fan J., Ding F. Materials Science and Engineering: A, **646** 315-321 (2015)
[8] Cadoni E., Dotta M. and Forni D. Procedia Structural Integrity **28**, 964 - 970 (2020)
[9] Cadoni E., Dotta M., Forni D., Tesio N., Albertini C. Materials and Design,**49** 657 - 666 (2013)
[10] Cadoni E., Dotta M., Forni D., Tesio N. Materials and Structures, **48** 1803-1813 (2015)
[11] Cadoni E., Singh N., Forni D., Singha M., Gupta N., The European Physical Journal Special Topics **225**(2) 409-420 (2016)
[12] Singh N.K., Cadoni E., Singha M. Gupta N.K. Journal of Engineering Mechanics ASCE **139** 1197-1206 (2013)
[13] Cadoni E., Dotta M., Forni D., Spaetig, P. Journal of Nuclear Materials **414** 360 - 366 (2011)
[14] Forni D., Chiaia B., Cadoni E., Materials and Design **94** 467-478 (2016)
[15] Cadoni, E., Forni, D. Fire Safety Journal, 102869 (2019)